

DEVELOPMENT OF A SET OF NUMERICAL HUMAN MODELS FOR SAFETY

Philippe Vezin

Jean Pierre Verriest*

*HUMOS2 project coordinator, on behalf of HUMOS2 consortium

INRETS, Biomechanics and Human Modeling Laboratory

France

ID (05-0163)

ABSTRACT

The objective of the EC funded HUMOS2 project is to develop Finite Element (FE) human models representing a large range of the European population and allowing an accurate injury risk prediction for victims involved in road accidents. A human model of a male in a driving position close to the 50th percentile – HUMOS model – resulting of the previous HUMOS project was presented (Robin [1]) at the ESV conference in 2001. The present paper focuses on the new developments that have been made in the still running HUMOS2 project.

Firstly, methods allowing the personalization (anthropometry, geometry and position) of human numerical models have been developed. They include a scaling tool enabling to derive any individual model from the original one through mesh control points and statistical relationships between external and internal dimensions. These were established from geometric data collected on standing and sitting human volunteers with a low dose bi-plane X ray system but also directly measured on isolated bone parts. A positioning tool has also been developed, based on a set of reference postures including seated car occupant, out of positions (OOPs) and pedestrian postures, in order to adjust and test the models for different sitting and standing postures.

Secondly, experimental work has been conducted on human volunteers in order to identify the influence of muscular tensing on body response to moderate impacts. A data base of biomechanical test results, appropriate for model validation, has been set up. It includes new biomaterial laws for ligament and skeletal muscles, as well as existing cadaver tests results coming from former EC projects and Heidelberg University. It and will be further completed by specific tests performed by consortium members. On-going work includes injury prediction rules introduction in the models then, extensive testing of the model in various conditions defined for validation.

INTRODUCTION

The European Union is the largest car producing area in the world and the largest car market. Research and Technological Development is essential for improving

the impact motor vehicles have on our society. Safety is one of the key issues in this respect.

In 2001, there were approximately 40,000 reported deaths and 1.6 millions casualties as a result of road traffic accidents in the European Union. The annual cost to the European Society due to these accidents was more than 160 billion Euro which was about twice the entire budget of the European Union. This situation increases with the integration of new state members. Injuries due to road accidents are a problem that can be controlled considerably if adequate attention is given to accident and injury prevention strategies. Injury control measures, i.e. passive safety, have been proven a very effective method for the reduction of the trauma problem.

The development of safety devices needs tools capable of predicting the injury risk and of evaluating the protection of road users (car occupants, pedestrians, two wheels users). For a long time, these tools have been only represented by mechanical crash test dummies. They were used for car safety research, development, and regulatory testing as well. These anthropometric crash dummies are limited in their biofidelity and in their application type. Moreover, the existing mechanical dummies represent only the population through 3 sizes (50th percentile male, 5th percentile female and 95th percentile male). Therefore, the crash test dummies produce important shortcomings with respect to a real crash situation.

Increasing computational capabilities have allowed designers to efficiently integrate simulation techniques into the conception cycle of their prototypes. This is also true for numerical models of crash test dummies, nowadays fully integrated into the crash simulation procedures. Unfortunately, these models inherit the deficiencies of their mechanical counterparts (i.e. biofidelity).

Moreover, there is an increasing interest on the possibility to use and introduce the “Virtual Testing” concept in the regulation and in the design process of safety devices, car or other transportation modes. This advanced approach requires more efficient, complex and biofidelic human substitutes. A global human body model capable to simulate the response of a human being and capable to predict the injuries in case of an omni-directional impact is one of the main keys of this new challenge.

The basic assumption of the project is that a biofidelic model shall be structurally close to the real human body. This assumption means that a correct representation of the human structures is needed, not only the bony parts but also the organs and muscles. Afterward, an up-to-date knowledge is also needed in order to provide the model with a satisfactory mechanical behavior in a car crash situation.

The second assumption of the HUMOS2 project is that all road users need to be correctly protected by the safety devices during a collision and consequently it is necessary to develop personalized models able to represent all the population. That means that, in parallel with the development of a biofidelic finite element human model, tools need to be developed for the “scaling”, i.e. personalization of the internal and external geometry, and for the “positioning” to obtain easily specific models for car occupants, pedestrian, motorcyclist, etc... from a reference model.

METHODS

The HUMOS2 program was organized around different tasks. *The two first tasks* aimed at providing meshes representative of the 5th percentile female and the 50th and 95th percentile male in sitting and standing positions. European databases of anthropometry measurements were therefore analyzed in order to define the external geometry of the human body corresponding to these percentiles. For the internal geometry, relationships between external dimensions and internal organ dimensions were established. The paired acquisition of internal dimensions (skeletal parts and some soft organs) and of external (anthropometric) measurements was performed on 64 volunteers by means of a low dose bi-plane X Ray imaging system [2] and on PMHS (Post Mortem Human Subject) by direct measurements. The collected data were analyzed by statistical methods in order to establish a scaling law for the prediction of internal organ dimensions from external ones. Thus, internal dimension of the 5th percentile female and the 50th and 95th percentile male derives from external geometry. Based on these statistical relations, a specific software was developed. This tool allows the scaling of the existing HUMOS mesh (close to the 50th percentile) towards any other percentile from a set of external main dimensions. It was used to produce the 5th, 50th and 95th percentiles in sitting positions. Before being scaled, the existing mesh (HUMOS) was improved in order to ensure its quality, especially after the scaling and positioning processes. This work was based on:

- identification of mesh defects during crash simulation (done by end users of the original model),
- needs identified by biomechanical experts for injury mechanisms simulation,

- needs identified for scaling and positioning purposes.

Specific road user postures were also defined for car occupants and pedestrians, using ergonomic and/or accident study data. Automatic methods were defined as positioning tool for small and for large displacements. From the meshes corresponding to the driving position (5th, 50th, 95th percentiles), other meshes were built for the pedestrian positions.

The third task deals with the improvement of biomechanical behavior knowledge specifically concerning the mechanical properties of biological tissues, the effect of muscle tone and the whole body response to realistic impact conditions. This knowledge is fundamental for the improvement and validation of the FE models.

Firstly, the effects of muscle tonicity on the global body response of volunteers subjected to impact and on local deformation of muscle were analyzed, as well as the effect of the muscular pre-activation. Secondly, mechanical characterization of soft tissues (muscles, tendons and ligaments) was performed. The mechanical properties of skeletal muscles during (impact) loading, up to failure were determined. Existing sled tests on PMHS were reanalyzed and new tests are being performed in more realistic impact conditions to validate the developed models. Effects of organs interaction during impact were determined thanks to the analysis of clinical records of visceral injuries, dissections and drop tests on trunks. Finally, all these biomechanical data will be stored in a biomechanical database necessary for the task dedicated to the models validation.

Task 4 deals firstly with the improvement of the developed models by simulating the injury mechanisms, the pressurization and the effect of muscle tone. For the simulation of injury occurrence, injury mechanisms were identified for each body parts. Behavioral laws for the tissue up to failure will be implemented and validated. The experimental data obtained on volunteers concerning the effect of muscle tone will be used for the development and the validation of active muscle models. Secondly, after the improvement of the whole body models, their biofidelity and injury prediction capabilities will be assessed by referring to the PMHS sled tests performed in the biomechanical study.

The last task is dedicated to an extensive use of the HUMOS validated models in different impact conditions in order to assess their capacity in predicting injuries. The simulation of car crash or other transport accident situations and of body response in case of out of position will be carried on. Another objective of this work is to compare these capabilities with dummies in view to complete the current regulations by numerical simulations.

GEOMETRY DEFINITON

Geometry Acquisition

In the field of product design, it is important to be able to represent the user population from the 5th percentile female to the 95th percentile male. Three dimensional data allowing geometrical reconstruction of any individual are therefore necessary. The “geometrical acquisition” work performed aimed at providing a database of external and internal measurements of the human body.

The external measurements concern more than 50 anthropometric lengths of body segment (on volunteers and PMHS in both standing and sitting positions). Data collected (Appendix 1) includes age, sex, weight, lengths, heights and circumferences.

Three-dimensional measurements of anatomical landmarks (acromions, trochanters, iliac crests, etc...) identifiable on the skin were performed in order to define the orientation of body segment in a sitting position. Their anatomical identification was simply done by palpation with the help of anatomists. Their 3D coordinates are expressed in a global frame attached to the subject. Other anatomical points were also acquired on volunteers in both standing and sitting position.

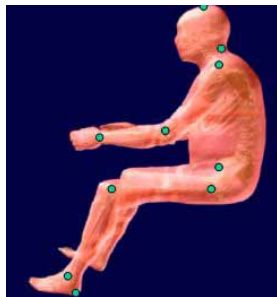


Figure 1. Palpable points (Doc. Univ. of Méditerranée).

The internal measurements related to anatomical points, which allow the description of the geometry of the organs. That concerned the head, the spine, the ribs and the sternum, the pelvis, the bones of the upper and lower limbs and the liver. For each organ, “control” points, dimensions based on these points and a local frame attached to the organ were defined. With the symmetry hypothesis, more than 1000 control points and 400 dimensions have been defined.

In order to define the relative position of each organ in the sitting position, all local anatomical frames were expressed in the global frame attached to the subject. Data were acquired on 64 volunteers (mean 30 ± 9 years old) distributed as 16 female, 33 and 15 male subjects representative of respectively the 5th, 50th and 95th percentile, (Table 1.). Data were also collected on 24 PMHS.

Table 1.
The 5th, 50th and 95th percentile definition

Percentile	Weight (Kg)	Standing height (cm)	Erect sitting height (cm)
5 th female	47	154	83
50 th male	77	178	94
95 th male	103	190	100

A common protocol was used to perform external measurements on volunteers and PMHS but different protocols were set up for internal data. The “*volunteer protocol*” is based on an X-ray acquisition using the low dose stereo X-rays system EOS[®] and on a 3D reconstruction procedure (Figure 2). Internal data concern the 3D points of the trunk skeleton (C3-L5 vertebrae, pelvis, 1st to 10th right and left ribs, sternum).

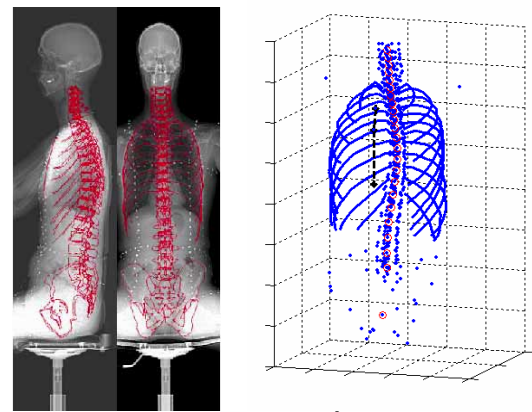


Figure 2. X-ray picture of a 50th male subject in sitting position and 3D control points obtained on a seated volunteer. Ribs are represented with lines joining 3D points (Doc. SERAM).

The “*PMHS protocol*” is based on 3D measurements of anatomical points on bones removed from PMHS. The study focused on limbs bones, head and sternum. In order to have some data on soft tissue organs, a specific protocol based on dual X-ray images was set-up to acquire data on the liver. An example of 3D control points is given in Figure 3.

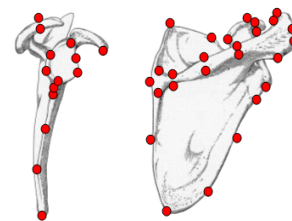


Figure 3. 3D control points measured on the scapula (Doc. INRETS).

These data were used to find statistical links between dimensions, inter or intra organ, and to give an approximate geometry of any percentile. The samples contained in the database are described in Table 2.

Table 2.
Description of the samples contained in the HUMOS2 Geometrical Database

Internal control points	Subjects	Samples
Head	11	21
Clavicle	14	18
Scapula	14	50
Humerus	23	32
Radius	14	24
Ulna	14	29
Femur	23	38
Tibia	23	30
Fibula	13	19
Sternum	73	3
Thorax	64	100
Pelvis	64	401
Liver	9	9
External dimensions	88	54
External control points	Samples	
Sitting position	64 trunks, 10 limbs	
Standing position	15 trunks	

Parameters Defining External/Internal Human Body Geometry

The European 5th, 50th and 95th percentile definitions given in Table 1 were determined from existing database analysis. For a p^{th} percentile, an arbitrary function δp , depending on weight (W_i), height (H_i), and erect sitting height (ESH_i) of a subject S_i was defined as follows (Eq. 1.):

$$\delta_p(S_i) = \frac{|W_p - W_i|}{W_p} + \frac{|H_p - H_i|}{H_p} + \frac{|ESH_p - ESH_i|}{ESH_p} \quad (1.)$$

The δp function was applied to all the subjects (volunteers and PMHS) in order to select among all of them the 3 subjects S_p with the smallest $\delta p(S_p)$. These subjects will be the target for the building of the different HUMOS2 percentile meshes.

Table 3 shows the subjects of the geometrical database whose anthropometry was the nearest (according to the δp criteria) to the percentile definitions.

The methodology chosen for the personalization of a numerical model, based on a “*scaling method*”, needs the definition of the links between external/external, external/internal or internal/internal dimensions. These correlations are the key data of the “*statistical tool*”, which provides from a small number of main

(external) parameters (input data) all the parameters (external and internal) defining the geometry of the considered person.

Table 3.
Subjects with the smallest δp value

Percentiles p		H_p (cm)	ESH_p (cm)	W_p (kg)
5 th female	PMHS	159.5	85.0	47.5
	Volunteers	155.9	83.0	46.9
50 th male	PMHS	179.0	82.0	72
	Volunteers	182.5	93.0	76.3
95 th male	PMHS	-	-	-
	Volunteers	189.4	97.1	98.5

The method comprised three steps which provide the three following output (Figure 4.):

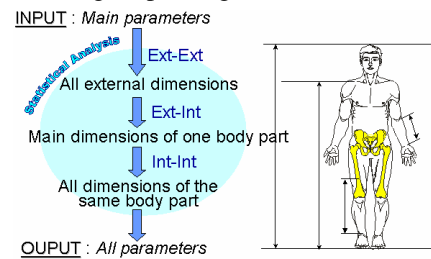


Figure 4. Regressive methodology (Doc. SERAM)

1. All external dimensions determined from main parameters by using external/external links;
2. The main dimensions of body parts from all external dimensions by the mean of external/internal links;
3. All dimensions of a body part from the main dimensions of the same body part by using internal/internal links.

Many correlations were found in the literature but the existing relationships do not meet to the HUMOS2 objective. Hence, the HUMOS2 geometrical database was analyzed by statistical methods in order to establish relationships between external anthropometric dimensions and internal organs dimensions. This work is based on:

1. The definition of MPE (Main External Parameters for the whole body or one body segment, MSE (Secondary External Measurement for one body segment), MPI (Main Internal Parameters for one body segment), and MSI (Secondary Internal Measurement for one body segment);
2. The definition of anthropometrical links: external/external (MPE/MPE, MPE/MSE), external/internal (MPE/MPI, MSE/MPI), and internal/internal (MPI/MPI, MPI/MSI);
3. The determination of correlation coefficient;
4. The determination of linear regressions.

Thanks to the statistical procedure, 285 linear regressions were assessed in order to model 285/411 (69%) parameters. Figure 5 describes the diagram of the statistical analysis which provides internal and external anthropometrical dimensions from 10 of the external measurements. It consists in 3 steps: 1) all the MSE are modeled thanks to 10 MPE; 2) 81 MPI and 30 MII (Isolated Internal Measurements) are modeled thanks to the MPE and the MSE; 3) 134 MSI are modeled thanks to the 81 MPI.

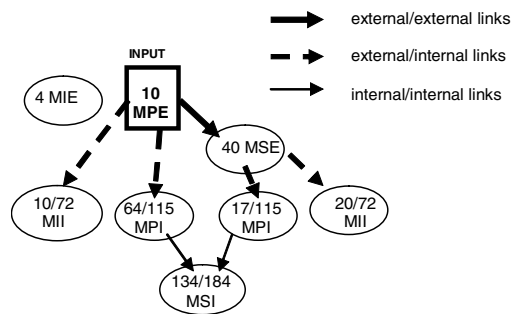


Figure 5. Statistical analysis summary (Doc. SERAM).

Given the small size of samples used to determine some regressions, some body part dimensions modeled by simple linear equations are less effective than others. Some internal parameters were not modeled by the statistical analysis as shown. This is due to the selection criteria used for the regressions ($R^2 > 0.5$) but it seems essential to get accurate predictions.

Methodology for Scaling

A specific tool was built allowing the “scaling” of the reference mesh (previous HUMOS 50th percentile) toward any other p -percentile and to validate it with the 3 common used percentiles (5th female, 50th and 95th male). These different HUMOS2 meshes are generated by the HUMOS2 “scaling tool” (Figure 6).

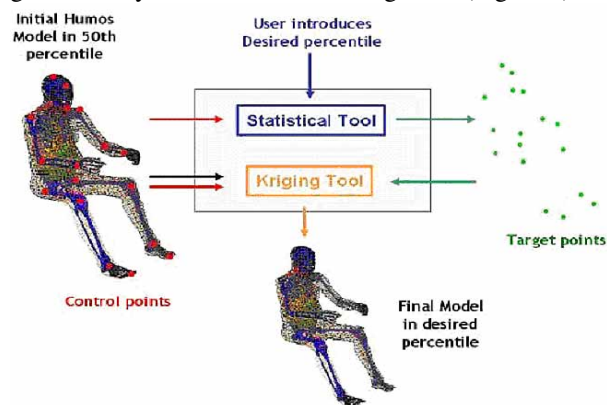


Figure 6. Main structure of HUMOS2 scaling tool. (Doc. Mecalog).

This tool uses the above-mentioned anthropometrical links and the “control points” defined on the initial HUMOS mesh (the “control points” have the same location as those measured on the volunteers and PMHS). From the 10 main parameters of a desired p -percentile, the “statistical” part of the tool determines the “target points” of this p -percentile. Then, using a method based on the kriging method the mesh of this desired p -percentile is created.

Consequently, the scaling of HUMOS2 mesh into any percentile in driving position is realized through a single step and requires only 10 anthropometrical dimensions. An example of the 5th female, 50th and 95th percentile male obtained from HUMOS mesh with this scaling tool is given in Figure 7 .

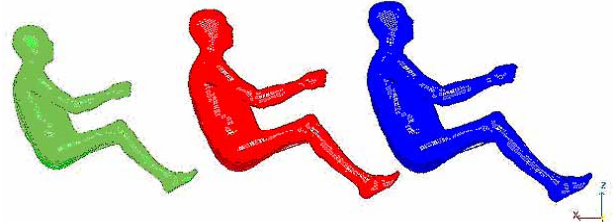


Figure 7. Example of the different HUMOS2 percentile (Doc. Mecalog).

MESHES UPDATE

Before proceeding to the scaling, the HUMOS model was exhaustively analyzed in order to define and select model which segments have to be improved via mesh improvements conditioned by 3 elements:

- Identification of HUMOS mesh defects during crash simulation conducted by end-users,
- Requirements for injury mechanisms simulation,
- Requirements for the scaling and positioning of the initial model.

The following improvements have been made:

Head and Brain Meshes

Brain Modeling: In order to predict the brain movement and brain vessel failure, the skull needed first to be separated from the brain. The skull is meshed using shell elements, which means that there is no physical thickness of the skull bone structure. For that reason the intracranial space was directly connected to the skull by sharing the same (joined) nodes. After the separation, the positions of the nodes are still the same but the nodes are no longer attached.

Bridging Veins Implementation: Because of the bridging veins introduction in the head model, the brain was repositioned and scaled such that the veins are more realistically positioned and orientated..

Anatomy handbooks show that the average distance between skull and brain is 1.4 mm and this space is filled with fluid (CSF). The intracranial space of the model was scaled to get this correct average distance. A layer between the brain and bone skull inner "surface" is also needed to get a better prediction of the bridging vein failure during crash. Rupture of these veins results in Subdural Hematomas, which are one of the most important causes of fatal head injuries. Figure 8 shows the skin shell (light brown), the head flesh solid (brown transparent), the bone skull shell layers (blue) and the intracranial space (red) with in between the veins (yellow).

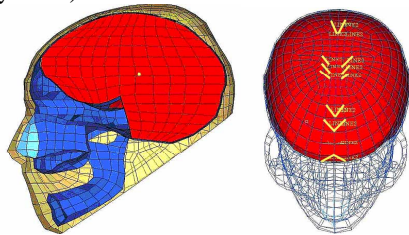


Figure 8. New head model with intracranial space and bridging veins (Doc. TNO).

Neck Improvement

Neck Geometry Modification: The geometry and corresponding mesh of the neck of the HUMOS model needed some modifications to achieve a more biofidelic performance. The relative angle between C3 and C4 was found to be out of range for normal values, 23.8° instead of 6.6°, Harrison et al. 0[3], and needed correction. The relative angle between C2-C7 for HUMOS is larger than an average neck but was kept to avoid important changes at this stage. The global curvature of the neck was adjusted to a better distribution of the vertebrae and cervical discs, C3-C6 were individually rotated around a local transverse axis, at the rear lower part of the vertebra body. The relative angles between the adjacent vertebrae were also defined within the range given by Harrison.

Neck Mesh Modification: After rotation of the vertebrae, the mesh of the pedicles and the spinous processes were modified to give the global neck model a smoother curvature. The facets also follow the new orientation of the pedicles. The comparison of the old and new neck is shown in Figure 9. The meshes of spine disc and nucleus pulposus were modified for a better size distribution within the solid elements and are modeled with two elements over the height and adjusted by placing the mid-layer-nodes at half distance between the upper and lower surface nodes.

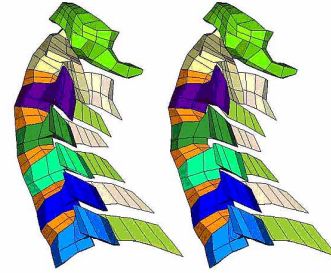


Figure 9. (left) Old geometry, (right) modified model with smoother curvature (Doc. Volvo).

Upper Limb

Elbow Mesh Refinement: In order to get a good contact description between the components of the elbow, refinement of the bones was needed. The meshes of the attached components were adapted as shown in Figure 10. From the available surfaces it was not possible to re-mesh the components to make them more realistic (smooth surface rounding instead of the edge formed surfaces). The number of shell elements was increased from 225 to 877 to have a denser mesh.

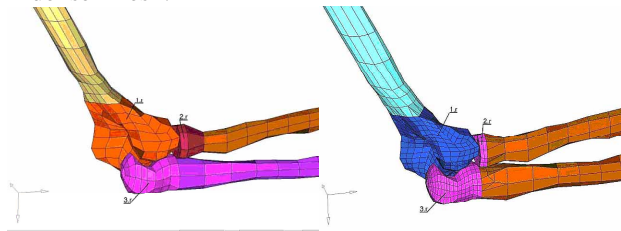


Figure 10. Elbow mesh refinement, left) old; right) new (Doc. TNO).

Elbow Ligaments Implementation: In order to be able to predict the movement of upper and lower arm through contact descriptions in the elbow, ligaments are necessary to keep the different components positioned correctly with respect to each other. Four ligaments, CollUlnar, AnnuRadial, CollRadial and Quadrate-R, were added in the refined mesh and therefore were adapted to the new mesh density. Figure 11 shows an example of two of the four added ligaments on right elbow with the denser mesh.

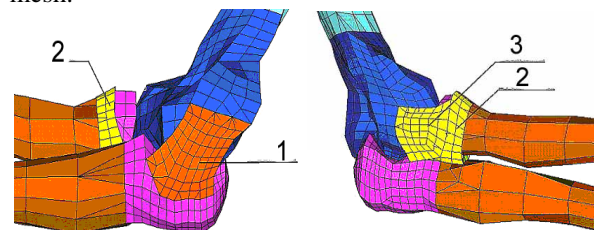


Figure 11. Elbow mesh with ligament CollUlnar 1), AnnuRadial 2) and CollRadial 3) (Doc. TNO).

Thorax, Abdomen, Pelvis

Ribs Mesh Improvement: To predict the rib injury with greater accuracy, the ribs mesh has been refined. Figure 12 shows the ribcage before (left) and after (right) refinement of the cortical (shells) and the trabecular (solids) bones. Each element has been divided into two elements along the curvature of the rib. The refined rib cage is now composed of 5518 shells and 2796 solids.

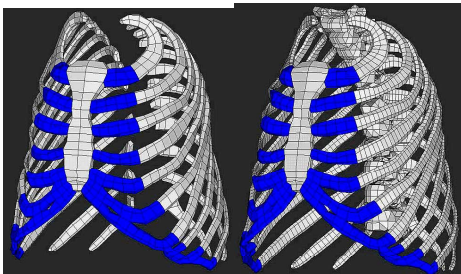


Figure 12. (left) Old, (right) new ribs mesh (Doc. ESI).

Aorta Insertion: The aorta rupture is an important injury of the thorax. The mesh of this organ has been added in the model. The geometry of the aorta came from unused data of the previous HUMOS project. It has been transformed to obtain an adequate position with respect to the heart, the spine and the diaphragm mesh. Figure 13 shows the mesh with shell elements of the aorta between the heart and the diaphragm.

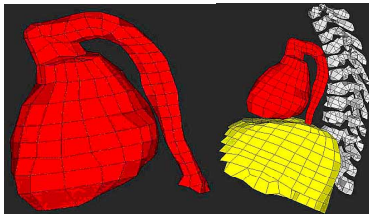


Figure 13. Aorta mesh (Doc. ESI).

The mesh of the aorta is composed of 191 shells and is connected to the heart and to the diaphragm by a continuous mesh. It is superimposed to the flesh for connection between organs. Thus, no interaction between the aorta and the flesh is possible through the mesh. An attachment between the aorta and the spine and a contact between the aorta and the lungs, the heart, and the spine has still to be modeled.

Thoracic and Abdominal Organs Mesh Improvements: The mesh quality of the thoracic and abdominal organs has been checked and corrected. The liver, the stomach and the intestines mesh have been corrected, but the maximum angle criteria (mesh quality criteria) were partially respected because of the specific geometry of those organs. In the first HUMOS model, the mesh of the heart, the lungs and the flesh were continuous. In the updated version, the heart mesh has been separated from the flesh and from the

lungs to allow the relative motion of the heart with respect to the lungs. This part of the model needs further development concerning the description of the organs and soft tissues, especially in the abdomen

Lower Limb

Lower Limbs Bones Improvements: The femur and tibia cortical bones were refined to improve the response of lower limbs and to predict bone fracture. Each element has been divided into two elements along the bone long axis. The refined femur and tibia bones are respectively composed of 220 and 176 shells. The capsular hip joint, composed of 16 1D elements, has been added between the femoral head and the Glena (Figure 14) to improve the hip model.

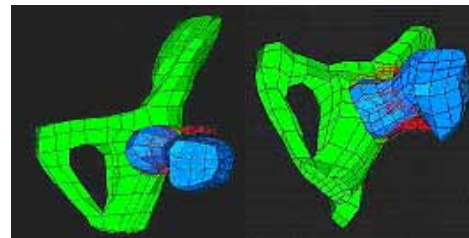


Figure 14. Capsular hip joint (Doc. Mecalog).

Lower Limbs Flesh Modifications: To improve the response of the model in terms of soft tissue/bone contact and to reproduce more precisely the behavior of pedestrian, refinements were performed on the flesh and skin of lower limbs.

Figure 15 shows the new mesh of the knee. For the limbs, the meshes are composed respectively of 1559 solids and 914 shells elements (787 solids and 573 shells elements for the old flesh and skin version).

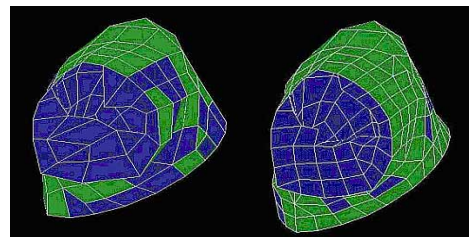


Figure 15. Upper leg and knee flesh (blue) & skin (green), left) old; right) new (Doc. Mecalog).

POSTURE DEFINITION

Standard Occupant Position

The occupant of a car involved in an accident can be a driver, a passenger front seat or a passenger rear seat. Defining correctly these various occupants' positions is a need for an accurate injury prediction. The occupant morphology was also taken into account. For each case the best ergonomic posture was studied. It was proposed to use DSPM [Driver

- In about 85% of the cases the pedestrians were hit laterally (37% at the right side, 48% left);
- 15% of the pedestrians are struck on their front;
- 79% of the pedestrian were in motion;

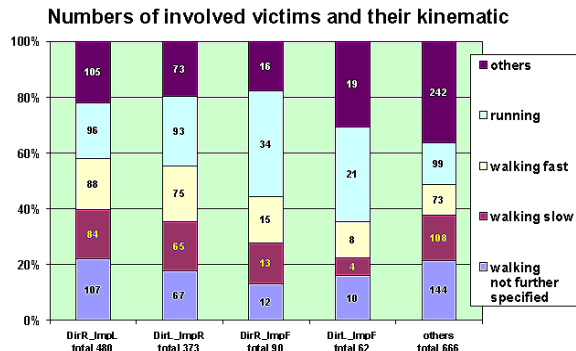


Figure 19. The numbers of involved victims and their initial moving postures (Doc. VW).

Then, an investigation was performed with 35 well-documented fatal cases of pedestrian/vehicle accidents which were reconstructed. The typical positions in real accidents with location of the first contact interaction and the produced injury by this contact were analyzed. The analysis pointed out that:

- for most of the pedestrian/car accident cases, the pedestrian was hit while crossing the road in an upright position;
- the 1st contact interaction of an adult is most frequently located at the lower extremity especially the shank, according to the bumper height of the involved car;
- there is a correlation of normal gait cycle with pedestrian initial posture.

The pedestrian postures in front of the vehicle before the impact were analyzed based on accident data:

- For the walking position, it was proposed to take into account the leg orientation. During the pedestrian impact, the kinematics and dynamic loading of pedestrian are not the same if the left leg is forward or if the right leg is forward;
- Concerning the running position, it is difficult to validate a pedestrian model due to the lack of physical test data available in this configuration;

Based on the results from this study, it was concluded that the impact responses and injury outcomes are significantly affected by the initial postures and the orientation of body segments. The consortium agreed to develop two pedestrian models. One model is in normal standing posture and another in normal walking posture. The positioning of the pedestrian model is defined based on the anatomical position of human body (Figure 20).

The postures of the pedestrian models are to be adjusted according to the configuration of the needs in specific modeling of vehicle/pedestrian impact.

The normal walking and running postures with left leg forward are specified with related rotation of joints from the baseline model within the range of physiological movement (Figure 20).

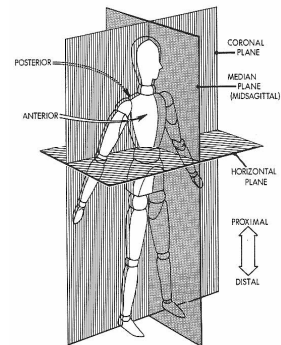


Figure 20. Anatomical position of the human body, baseline model.

Table 4. Rotation from normal standing to walking and running posture

Body segment	Walking	Running
Left hip flexion	6°	6°
Right hip extension	6°	5°
Left knee flexion	3°	8°
Right knee flexion	5°	35°
Left elbow flexion	6°	80°
Right elbow flexion	4°	69°
Left shoulder joint	8°	23.5°
Right shoulder joint	8°	15°
Left ankle extension	3°	-
Right ankle flexion	2°	-

Positioning Tool

The meshes of 5th, 50th and 95th percentiles in the pedestrian and car occupant positions will be created from the corresponding meshes in sitting position. To achieve these objectives a positioning tool is under development. Preliminary simulations were performed to study HUMOS capability to be in standing position and shown satisfactory results even if a re-mesh of pelvis flesh in standing position are necessary.

Each software developer involved in the development of the HUMOS2 models builds its own positioning tool based on different approaches.

For example the positioning tool developed by ESI uses interactive real-time background calculations provided by a simplified finite element solver (SFE solver). The main feature of this positioning tool is to model the physics needed during user imposed articulation movements. It does this by:

- performing real time simulation,
- using rigid body dynamics and joint physics in the simulation,
- imposing user requested rotations and translations,
- using other physics based options such as elastic structures and contact interfaces,
- using geometry based options such as geometrical interpolation.

An example of results from the positioning tool developed by ESI is shown in the following Figure 21 and compared with the position of a car occupant as defined in “car occupant definition” work.



Figure 21. HUMOS2 model in posture of 50th percentile driver compared with the standard car occupant position (Doc. ESI).

The method used by Mecalog.in its positioning tool software allows setting any percentile model in any position without calculation. By using a pre-calculated position database, a new position can be computed by using only linear interpolations. The specification of the wanted position by the input of 28 angles allows a quick, easy and reliable use of the software. Figure 22 shows an example of the different leg position obtained from the software.

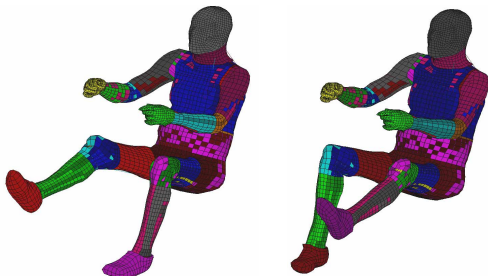


Figure 22: Different leg positions for a 50th percentile obtained from the Mecalog positioning tool (Doc. Mecalog).

TISSUE MECHANICAL PROPERTIES

Biological Material Laws

The assessment of injury risks and the prediction of injuries need the implementation in the model of up-to-date material properties. Soft tissues, in particular muscle material properties at high loading rate are poorly described in the literature. Consequently, some experimental static and dynamic tests were achieved

within the project on different biological materials such as ligaments and skeletal muscle.

Dynamic Behavior of Ligaments: The goal of this research was to characterize the mechanical behavior of soft tissues under a wide range of loadings (from quasi-static to dynamic). A protocol was designed for performing tensile tests on knee ligaments placed in a *physiological* position. The experiments deal with cyclic and failure tests, under quasi-static and dynamic loadings of the PCL (Posterior Cruciate Ligament) and LCL (Lateral Collateral Ligament). The same protocol was used for the two types of loading. (Figure 23.)



Figure 23. Pictures of the sample placed on the tensile device (Univ. of Méditerranée).

Cyclic tests were performed with prescribed displacement at the frequencies: 10, 20 and 30 Hz, and amplitudes of displacement: 1, 2 and 3 mm, and with sinus or triangle displacements. Speed range was then from 20 mm/s to 180 mm/s. The knees were first cyclically tested with the 2 ligaments, then one of them was removed. Finally, the other ligament was tested up to failure. Tests were beside performed for 2 angles of knee flexion (180° and 120°).

The comparison of ligaments behavior shows that:

- The dissipation during cyclic tests is independent on the frequency, that is to say on the velocity,
- The ranges of load for the cyclic tests are not very different in quasi-static and in dynamic,
- For the failure tests, the stiffness of the PCL in flexion and of the PCL in extension are only a bit higher in dynamic than is quasi-static, whereas the failure loads and failure displacements are clearly higher in dynamic than in quasi-static,
- The failure occurs mainly at the insertion sites, and it is deeper in dynamic than in quasi-static. In dynamic, there is always a loss of cohesion in the ligament, whereas this was not observed for the quasi-static tests, at least at the macroscopic level.

Finally, from the results, numerical laws are proposed for the behavior of the ligaments and will be implemented in the HUMOS2 models.

Dynamic Muscle Properties: There is only few data available on the behavior of skeletal muscle under dynamic conditions. A study was then dedicated to improve this knowledge. The aim is to

determine the transverse mechanical (stiffness) properties of skeletal muscle at quasi-static loading and for dynamic loads up to high frequencies. A second objective is to find damage thresholds of the skeletal muscle, which can be used in crash tests.

The quasi-static properties were determined using in a non-invasive set-up that allows *in-vivo* determination of the properties of skeletal muscle in Brown Norway rats using a MRI-facility. Conceptually, the best way to determine properties is to do that *in-vivo*, because problems with making test-samples and keeping tissues in the proper conditions during *ex-vivo* testing can be avoided. Moreover, properties found are more representative for the real tissue than *ex-vivo* properties. Immediately after a load is applied and removed it is also possible to detect damage at the cell level by means of T2-weighted imaging (Figure 24).

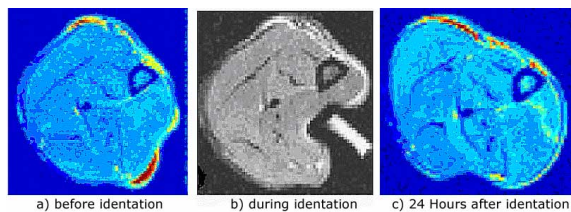


Figure 24. T2-maps of the rat hind limb. (Doc. TU Eindhoven).

The dynamics tests were performed *ex-vivo* with standard DMTA testing on a rheometer. In this case the disadvantages of *ex-vivo* testing were accepted, because of the possibility to use time-temperature superposition. By cooling down the samples and measuring at low temperatures, the properties change according to a specific time/temperature rule. Then, a master curve at the relevant temperature can be constructed for a broad range of frequencies. This procedure has been already performed for brain tissue with success (Brands et al. [8]) and could be used for skeletal muscle for frequencies $< 16\text{Hz}$.

From a comparison from quasi-static and dynamic experiments the following conclusions can be drawn:

- It appears that the shear stiffness increases to reach a plateau value of 40 kPa at high frequencies. Visco-elastic effects become very small at high frequencies.
- The muscle tissue behaves linear for shear strains up to $3 \cdot 10^{-3}$. The loss modulus decreases from with the frequencies. At high frequencies the material starts to behave as an elastic material.
- For small deformations the Neo-Hookean model is a suitable model for muscle. For large deformation the Ogden model has to be used. For details on the implementation of the Ogden model in a finite element code see Simo [9].
- It is acceptable to use elastic properties for skeletal muscles for impact studies with the HUMOS2 model.

Effect of Muscle Tonicity

The main limitation of current human models is the lack of data included about the effect of the muscle activities. Moreover, the models are often validated with data coming from cadaver tests without muscle tonicity. A tentative work was started in the project in order to obtain information on the effect of muscle tone on the global kinematics and on materials properties and to assess the influence of the muscle pre-activation on the response to a moderate impact.

Effects of Muscle Tone on the Kinematics: The first objective was to determine the effect of muscle tone on the response of the human body in lateral, dorsal and frontal thoracic impact by subjected volunteers to pendulum impact (Figure 25).



Figure 25. Impact locations lateral, dorsal and frontal (Doc. LMU).

The influence of muscle state was investigated by performing “unexpected” (relaxed muscles) and “expected” (pre-activated muscles) pendulum tests. Quantitative analysis of displacements (amplitude, time of beginning and maximum) and muscle activities (time of onset) resulted in mean values that can be used for validation of the HUMOS2 models.

The test setup fulfilled the following requirements:

- Used of volunteers with minimal risks of injuries;
- Application of experimental results for simulation;
- “Simple” modeling of test setup for simulation.

The kinematics were recorded by a motion analysis system using reflecting markers, the muscle activity was recorded by surface electrodes. The following parameters were quantified and used for the validation of the human models by comparing the experimental results with results from the simulation:

- Displacement in the impact direction for head-top and C7 markers;
- Angle of the head relative to the trunk;
- Onset times for left and right different muscles.

Measurements with different “height of deflection” and “weight of pendulum” were performed. An example of some results is given hereafter:

- Head-top and C7 displacements are less for tensed muscles than for relaxed muscles. Due to inertia the head shows a small displacement in opposite impact direction before the head is accelerated together with the trunk in impact direction.
- For higher energies, larger displacements and angles can be observed.

- High impact energy causes higher and faster muscle responses. Trunk muscles are activated later than neck muscles for side and rear impact..
- Displacements and angles show a higher variance for tests with relaxed muscles than for those with activated muscles. However, displacement curves for both muscle states appear similar for each volunteer (individual characteristics).
- For similar impulses in side impact, but twice the energy, similar displacements were found. Most likely, the impulse mainly influences the reaction or kinematics of the body.
- In rear impact, EMG onsets show a high variance and no correlation for the lowest energy. For higher impact energies the displacement is better correlated. In frontal impact, a good correlation is found for all impact intensities.

Effects of Muscle Tone on the Material Properties: The second objective was to determine the effect of muscle activation on the transverse material properties of the arm and femur soft tissue. Only few articles could be found investigating transversal material properties of muscle tissue. A test setup was therefore developed for the dynamic study of these properties in dependence of the muscle activation state. An impactor falls through a Plexiglas tube and impacts the volunteer's muscle (Figure 26).

Three impact locations were tested: 1) upper arm ventral, m. biceps brachii ; 2) upper leg ventral, m. quadriceps femoris, pars rectus femoris ; 3) upper leg dorsal, m. biceps femoris.



Figure 26. Experimental setup (Doc. LMU).

Peak accelerations, rebound heights, indentations and velocities were obtained. EMG signals of the muscle were recorded in order to get the muscle activity during the impact. The main results are:

- 1) Acceleration peak values for different activation states at a constant falling height nearly coincide.
- 2) Acceleration peak values vary between volunteers for relaxed muscles, but remain nearly constant for repeated tests with the same volunteer.
- 3) An increasing height of fall causes higher acceleration peak values.
- 4) First acceleration peak exhibits a distinct shape for relaxed and tensed arm muscles. This phenomenon could only be observed for the arm muscle, not for the leg. This might be caused by the difficult impact location definition.

- 5) For relaxed muscles no impactor rebounds were observed. The whole impact energy is transformed into flesh deformation. For tensed muscles several impactor rebounds are observed. The time between the first and the second acceleration peak (rebound peak) can be used for calculating the amount of energy transformed into deformation of the flesh.

Influence of Muscle Pre-activation: The third objective was to define the influence of muscular activation prior to impact (pre-activation) on the overall stiffness of the lower limb and to establish the relationships between this muscular activation prior to impact and impact loading associated with shock wave transmission from the shank to the thigh.

To establish these relationships, experiments were carried out using volunteers and a sledge ergometer (Figure 27). Such device allows to impact to the lower extremity of the seated subject while controlling the level of pre-activation. The evolution of the reaction force developed at impact, the corresponding variation of loading rates, the muscular force around the impact time (at and after), the associated kinematics of the lower limb and the impact cushioning provided by them were assessed.



Figure 27. Sledge ergometer (Doc. Univ. of Méditerranée).

The positive relationship between, on the one hand, the level of pre-activation and the impact peak force and, on the other hand, the associated loading and unloading rates were demonstrated. In others words, the increase of pre-activation generates the increase of the force-related parameters (impact peak force and associated loading and unloading rates).

It was tried to show the existence of differentiated reflex mechanisms with the increase of voluntary muscular pre-activation for the lower limb muscles controlling the thigh and leg dynamics.

On a functional point of view, it is evident that the driver tends to increase the overall stiffness of the lower extremity via muscular activation when a frontal collision is imminent and visible. The consequences of the increased pre-activation are:

- increase of the amplitude of the impact peak force with a higher loading rate,
- increase of reflex facilitation,

- the knee is the most controlled joint due to the predominant action of the Vastus medialis muscle compared to Triceps surae.
- massive attenuation of highest frequency components.

These results strengthen the point that it is necessary to include in human numerical models the muscle behavior to better evaluate the overall stiffness of the body before and at impact. The improvement of the biofidelity of the numerical models will allow the development of passive and especially active security devices in the automotive domain.

Global Validation Data

Finally, the whole human body models need to be globally validated in a situation representative of a real car crash. First validation data from sled tests were obtained in the first HUMOS project (Vezin et al. [10]). In HUMOS2 the acquisition of validation data is pursued through the re-analysis of existing data and by performing new test in frontal and oblique directions with up-to-date restraint systems. All these data and the information coming from the human material properties research will be gathered in a "Biomechanical Experiment Database" that allows the exchange of information between data suppliers and end-users of these information.

Existing sled tests analysis: The first objective was to re-analyze 46 frontal impact cadaver sled tests, performed at Univ. of Heidelberg, with belt and/or airbag protected subjects.

The tests were distributed in 4 test groups:

- 1st: 30kph, medium sled deceleration 20G, 11 tests
- 2nd: 40kph, medium sled deceleration 20G, 11 tests
- 3rd: 50kph, medium sled deceleration 20G, 12 tests
- 4th: 60kph, medium sled deceleration 15G, 12 tests

The analysis concerned: test conditions, anthropometric data for each case, time-histories of single and resultant signals, corridors, photographs prior to and after the test, medical findings in word protocol and schematic with classification according to AIS and digitized high-speed films.

Moreover acceptable correlations were found between mechanical parameters and injury severity:

- max. shoulder belt force vs. weight;
- max. shoulder belt force vs. weight x seating height;
- max. shoulder belt force vs. seating height;
- max. shoulder belt force vs. chest circumference;
- area below force-deflection curve vs. impact velocity.

Complementary sled tests: To further extend the validation database of the HUMOS2 models, new sled tests with PMHS are performed at INRETS. The goal of these experiments is to provide detailed information

on the global behavior of a body submitted to frontal and oblique impacts. Different impact conditions (50kph and 20G, 30kph and 15 G) and different restraint systems including load limited belt and airbag are being tested. A specific protocol was prepared by the Consortium and mainly focuses on the thorax behavior, but data about head, neck pelvis and lower legs will be provided.

Biomechanical Experiment Database

The objective is to develop a biomechanical experiment database which can gather the impact biomechanics results from experimental studies conducted with human subjects, either cadavers (donated to Science) or live volunteers. This research brings valuable results but is facing numerous difficulties due to various reasons: scientific, practical, technical and ethical. In some countries, this kind of research is very difficult to organize and sometimes is not possible at all. It is important to ensure the dissemination of these results as far as possible towards the scientific community in a way their use is facilitated. The european biomechanical experiment database will be established by the INRETS-LBMH Laboratory in order to properly disseminate and safeguard this data. The content includes data from biomechanical impact tests conducted in different laboratories involved in the project, as well as information on the associated test facilities and test subjects. The possibility to extend the content to the biomechanical experiments conducted within all EC funded RTD projects in the field of passive safety has been considered.

In the perspective of achieving this task, a list of specifications was drawn in order to establish the database. The opportunity was given to potential users of these data to express their needs (crash simulation code developers, dummy manufacturers, automobile manufacturers). Fruitful discussions conducted to several resolutions, among them the definition of guidelines for biomechanical testing depending on the use of the results (numerical model or dummy development). The database has been included into the activities of the European Advanced Passive Safety Network of Excellence, APSN, in order to guarantee its viability after the end of the project. This will provide at European level similar information as the existing NHTSA database in the US. The accessibility to the scientific community at large is also considered.

DISCUSSION AND CONCLUSIONS

In the view of designing widely accepted human body models, a joint effort between some European

car manufacturers, suppliers, software developers, public research institute and universities was undertaken since 1997 within the HUMOS project. The same participants and new partners, who provided expertise and knowledge in the field of biomechanics have decided to continue and increase this effort in the HUMOS2 project started at the end of 2002. This program led to the definition of a set of refined FE models of the human body in driving and pedestrian postures. These models were implemented with three main dynamic FE codes: Madymo[®], Radioss[®] and Pam-Crash[®]. This collaboration at a pre-competitive stage is very important to reach the common objective of designing a widely accepted model.

A large validation database was build and will be used to validate the models in different impact configurations. The injury predictive capabilities implementation and the validation of the model still have to be done in the final step of the project. This validation will comprise the simulation of injury mechanisms mainly for the thorax, knee and lower legs. The simulation of influence of muscle tonicity based on the experimental work performed in the project will be performed. Some attempts will be done to simulate the effect of the inner pressure. Finally the models will be validated thanks to the data included in the biomechanical experiments database.

In parallel with this validation effort, the HUMOS2 models will be extensively used in different impact conditions in order to assess their capacity in predicting injuries in real accident scenario via simulated reconstructions. The simulation of car crash or other transport accident situations and of body response in case of out of position will be carried on. Another objective is to compare these capabilities with those of the dummies in view to address the issue of introducing virtual testing with human models in the regulatory process.

Unfortunately, it is currently still difficult to account for the properties of living subjects, and as far as the mechanical behavior in car crash conditions is concerned, mainly cadaver results are available in the literature. In HUMOS2, a new step forward was done through the investigations on the muscle tone contribution and muscle pre-activation using volunteers tests. This research field is of great interest, especially for the low speed impact conditions that can be encountered in real field accident analysis. Furthermore, some limitations are due to the lack of knowledge of the injury mechanisms. The currently used criteria were implemented in the model, but its injury prediction capabilities are limited with regard to its complexity.

From the beginning of this research work, it was foreseen that some major limitations would remain. First of all, the geometrical definition of the model

despite its refinement, comes from a unique specimen, with some particularities. However, thanks to the geometrical acquisition work performed and scaling techniques, the HUMOS2 partners were able to define 1) a 50th percentile model from the current reference mesh and, 2) a 5th and a 95th percentile occupant models. They also derived from these models some pedestrian models. To achieve these innovations, two specific softwares were developed, one for the personalization of the model, i.e. “the scaling tool” one for the positioning of the models, “the positioning tool”. Obviously, these tools need further development, but within a very short term, they can provide the possibility to derive models of any living people in any postures possible during an accident occurring in any kind of transport mode.

It was also identified during this work that some knowledge is still missing as far as the soft tissues behavior is concerned, especially the abdomen needs a great attention in the future, and also the muscle tone contribution in some crash conditions. It is expected that the model itself, which is accounting for the main muscular structures and the main soft tissues will enable to carry out parametric studies aiming at evaluating the muscle contribution and aiming at the assessment of some injury mechanisms. In the future, Human models are called to play an important role in the development and validation of safety solutions through the use of virtual testing. Standardization and regulation bodies (ISO, EEVC) are presently looking at the potential for virtual testing to be used in a regulatory context. HUMOS2 is willing to support this process and may bring interesting tools besides those developed within other EC funded projects like VITES and ADVANCE. A lot of efforts is still needed for the development of the FE global human models; a new phase is about to start within the European funded Integrated Project “Advanced Protective Systems Project “APROSYSS.

CONTRIBUTING PARTNERS

The development of the HUMOS2 models is a joint effort of many partners. The coordination of the work was done by INRETS which was also involved in different parts of it. Univ. of Méditerranée coordinated the geometrical acquisition task and in collaboration with SERAM and INRETS performed an innovative work on the paired acquisition and analysis of internal and external dimensions of the human body. This was a very difficult and crucial work and the data obtained are of great interest for the research in biomechanics. Mecalog, with Univ. of Méditerranée developed the scaling tool for the personalization of the models.

Software developers were strongly involved in this research program. Mecalog (Radioss software) coordinated the meshing activities and insured the assembly of the final model with Radioss. ESI (Pam-Crash software) participated to meshing activities and was responsible of the validation task of the models. ESI also insured the assembly of the final model with Pam-Crash. TNO carried out the meshing and modeling work under the Madymo software and coordinated the human mechanical properties work. These three software companies have developed their own positioning tool during the project.

The car manufacturers involved were Volvo (neck re-meshing, validation and evaluation activities), PSA, Renault (evaluation work) and VW (definition of the positions, validation and evaluation tasks). The supplier Faurecia carried out the investigation of car occupant and pedestrian positions and participated to the evaluation and validation effort.

Chalmers University achieved a wide bibliographical study on the knowledge about injury mechanisms and contributed to the validation and evaluation of the models. Univ. of Heidelberg provided a deep re-analysis of full-scale sled tests with human substitutes including injury mechanism and contributed to the extension of the validation database. INRETS carried out complementary sled tests with human substitutes and contributed to the creation and the extension of the validation database. TU Eindhoven, and Univ. of Méditerranée carried out a research work aiming at defining of physical material laws under loading conditions for the different human soft tissues. The effect of muscle tonicity and pre-crash activities were studied through an innovative program of volunteer tests by Univ. of Méditerranée and LMU Muenchen. LMU participated also to the thoracic injury mechanism study, pedestrian position definition and to the validation and evaluation of the models. All these partners delivered a wide set of new experiments and contributed to the extension of the validation database.

ACKNOWLEDGEMENT

This project is funded by the European Commission under the 'Competitive and Sustainable Growth' Programme (1998-2002). The authors would like to thank to Ms. Liliane Pereira-Bahia and Mr. Loic Courtot for their essential help and contribution to the day-to-day management of this project.

REFERENCES

[1] Robin (2001). HUMOS: Human model for safety – A joint effort towards the development of refined human-like car occupant models. Proc. of the 17th Int.

Tech. Conf. on the Enhanced Safety of Vehicles, Paper Number 297.

[2] Kalifa G., Charpak Y., Maccia C., Fery-Lemonnier E., Bloch J., Boussard J.M., Attal M., Dubousset J., Adamsbaum C. (1998), Evaluation of a new low-dose digital x-ray device: first dosimetric and clinical results in children. *Pediatr Radiol* 28, 1998, pp 557-561.

[3] Harrison D.D. et al (1996). Comparisons of lordotic cervical spine curvatures to a theoretical ideal model of the static sagittal cervical spine, *SPINE*, 21 (6) 667-67.

[4] Appel, H., Stürtz, G. and Gotzen, L. (1975) Influence of impact speed & vehicle parameter on injuries of children and adults in pedestrian accidents. Proc. of the 2nd Int. Conf. on Biomechanics of Serious Trauma. Birmingham, England. pp. 83-110.

[5] EEVC (1982) Pedestrian injury accidents. Proc. of the 9th Int. Tech. Conf. on Experimental Safety Vehicles, pp. 638 – 671.

[6] EEVC (1998) Improved test methods to evaluate pedestrian protection afforded by passenger cars, Report, EEVC, WG17.

[7] Mizuno, (2003) Summary of IHRA pedestrian safety WG Activities (2003) - Proposed test methods to evaluate pedestrian protection afforded by passenger cars, Proc. 18th Int. Technical Conf. on Enhanced Safety Vehicle, pp.1-17.

[8] Brands D.W.A., Bovendeerd P.H.M., Peters G.W.M., Wismans J.S.H.M., (2000). The large shear strain dynamic behavior of in-vitro porcine brain tissue and a silicone gel model material, *Stapp Car Crash Journal*, Vol. 44, pp. 249-260.

[9] Simo J.C., (1987). On a fully three-dimensional finite-strain viscoelastic damage model: Formulation and computational aspects, *Computer Methods in Applied Mechanics and Engineering*, 60 pp. 153-173.

[10] Vezin P., Bermond F., Bouquet R., Bruyere K., Ramet M., Verriest J.P., Voiglio E. (2001). Comparison of head and thorax cadaver and Hybrid III response to a frontal sled deceleration for the validation of a car occupant mathematical model. Proc. of the 17th Int. Tech. Conf. on the Enhanced Safety of Vehicles, Paper No 114.

APPENDIX A

Table A1.
List of anthropometric measurements

1	Height (vertex - ground height)	26 c	Head maximum width
2	Eyes - ground height (Frankfort's plane parallel to the ground)	27	Head circumference passing over the glabella and through the occiput
3	Acromion (superior border) - ground height	28	Chin - occipital circumference (with lower jaw closed)
4	Elbow - ground height	29	Neck circumference under the thyroid cartilage
5	Anterior-superior iliac crest - ground height	30	Abdominal width (navel) (in sitting position)
6	Greater trochanter top - ground height	31	Abdominal circumference (navel) (in sitting position)
7	Knee articular interline spacing - ground height	32	Oblic circumference of the pelvis (going through the pubis cranial edge and EIPS, in sitting pos.)
8	Iliac bi-crest width	32bis	Thickness of buttock (pubis level, in sitting and standing pos.)
9	Bi-trochanter width	33	Abdominal thickness (navel) (in sitting pos.)
10	Sitting height (vertex - seat)	34	Buttock - heel length (tense leg)
11	Eyes - seat height (Frankfort's plane parallel to the ground)	35	Low pelvic circumference (going through the trochanters) (in standing pos.)
12	Acromion - seat height	36	Thigh upper circumference (superior third of 6-7 length)
13	Elbow - seat height	37	Thigh bottom circumference (inferior third of 6-7 length)
14	Cervical (C7) - seat height	38	Knee circumference (interline spacing level)
15	Bi-acromial width (between the 2 lateral borders)	39	Greatest calf circumference
16	Knee - ground height	40	Smallest ankle circumference
17	Buttock (backrest)- Knee length	41	Greatest foot width
18	Forearm length (olecranon - ulnar styloid with zero rotation of the hand)	42	Greatest foot length
19	Arm length (acromion (superior border) - 90°-flexed elbow) = middle of (12-13, 3-4) (calculated)	43	Lateral maleolus top (point the most lateral) - ground height
20	Thoracic axillary width (end of the exhalation) (in sitting pos.)	44	Arm upper circumference (superior third of 19 length)
21	Thoracic axillary thickness (end of the exhalation) for female subject without bosom (in sitting position)	46	Sternum length (without the xiphoid)
22	Thoracic axillary circumference (end of the exhalation) (sitting pos.)	47	Xiphoid angle (a, b, c) (tangent with the cartilage)
23	Thoracic sub-sternal width (end of the exhalation) (sitting pos.)	48	Longest hand length
24	Thoracic sub-sternal thickness (end of the exhalation) (sitting pos.)	49	Arm bottom circumference (inferior third of 19 length)
25	Thoracic sub-sternal circumference (end of the exhalation) (sitting pos.)	50	Greatest forearm circumference
26 a	Head length = glabella - occiput distance	51	Smallest forearm circumference
26 b	Skull height = auricular height (porion - vertex)		